Indian Journal of Engineering & Materials Sciences
Vol. 27, August 2020, pp. 853-859

# Buckling load for telescopic cylinder using successive approximation method

Sumit Kumar Gupta, Jatin Prakash & Pavan Kumar Kankar*

System Dynamics Lab, Discipline of Mechanical Engineering, Indian Institute of Technology Indore, Indore 453 552, Madhya Pradesh, India

*Received: 26 May 2020*

In this manuscript, a new way of determining the buckling load of the two-stage both end-hinged, single acting hydraulic cylinder has been engrossed using successive approximation method. The method has been extended from single stage hydraulic cylinder to the two-stage hydraulic cylinder mounted with pin support at both ends. This method includes a few numbers of iterations required in order to achieve good accuracy or in other words getting the minimum error. Further, finite element analysis of the hydraulic cylinder has also been performed for the validation purpose. The buckling mode shape for three different modes and their corresponding buckling load has also been obtained using the finite element method. The approximation of the buckling load corresponding to the first buckling mode shape has been performed and observed load lies in the close vicinity of theoretical calculation. The critical load obtained using a successive approximation method after two iteration shows the minor deviation of 3.63%.

**Keywords:** Hydraulic cylinder, buckling, Successive approximation method, Finite element analysis

## 1 Introduction

The hydraulic cylinder is a mechanical actuator majorly consisting of cylinder barrel and piston rod. It is widely used in dumpers, cranes and missile tilt. The failure analysis of particularly hydraulic cylinder has not been much focused. Hoblit was the first pioneer to find out the stability analysis of single-stage pin-mounted hydraulic cylinder considering it as a structural element and mathematically calculated the load-bearing capacity load up to the extent of stability[1]. Hobbit considered the buckling load for a fluid column is the same as for a solid column having the same length and moment of inertia. Flugge introduced the effect of fluid pressure inside the cylinder on the buckling load and thus treated it as a fluid column[2]. Seshasai *et al.* discussed the various stresses in the hydraulic cylinders[3]. The ISO/TS 13725(2001) standard explicated a method to determine the cylinder buckling load for a single-stage hydraulic cylinder[4]. Prakash *et al.* explained the analytical method to calculate the maximum permissible load for a hydraulic cylinder with both ends pin-mounted for single-stage and two-stage hydraulic cylinders[5,6]. It also discusses the effect of stresses in the cylinder considering thin and thick cylinder theory. It concludes that the piston rod is more prone to buckle due to the less flexural rigidity. Ramaswamy and Bash a discuss the effect of internal clearance using strain energy method and approximated with finite element analysis of multistage three-stage hydraulic cylinder[7]. The energy methods always give a value for the critical load which is higher than the true values[8]. Shariati *et al.* studied the effects of length and boundary condition on the buckling and post-buckling behaviour of cylindrical panels[9]. Raju and Rao demonstrated a methodology to determine the critical loads of uniform cantilever column employing two-term Galerkin method[10].

Thus, in this work, an approach called Successive Approximation has been adopted and modified to implement in the determination of buckling load for two stage hydraulic cylinders. The method of successive approximations provides a means of obtaining both lower and upper bounds of the critical load. Thus, the accuracy of the approximate solution is known, and the successive approximation procedure can be continued until the desired accuracy is obtained. The finite element simulation has also been performed for the approximation of the proposed methodology.

## 2 Mathematical modelling: Successive approximation method

Successive approximation method is a useful way to determine the buckling load of a bar having different cross-section[8]. Thus, in the ongoing study, this method has been modified and adapted to

*Corresponding author (E-mail: pkankar@iiti.ac.in)

determine the buckling load of the two-stage, single-acting hydraulic cylinder with both ends pin-mounted. The cylinder tube has been divided into 18 parts of equal length $\frac{l}{18}$. Because of the symmetry about Y-axis, the analysis can be done considering only half of the section as shown in Fig. 1. The ratio of the second moment of the area of a piston rod and the cylinder barrel 1 $(I_1/I_3)$ is found to be 0.1142 whereas that of $(I_2/I_3)$ is 0.2867. Table 1 shows the dimensions of the considered hydraulic cylinder.

The deflection curve equation $(y_1)$ used for the first approximation for the buckled rod is given by the parabolic equation as shown in Eq. (1).

$$y_1 = \frac{4\delta x(l-x)}{l^2} \quad \ldots (1)$$

We know that the bending moment at any section of the bar is $M_i = Py_i$, where, P is the axial force.

In the next step, $M_1/EI_i$ is tabulated which represents the load intensity on the conjugate beam at the station points. These values are given by $Py_1/EI_i$.

To calculate the concentrated load at different stations, two different methodologies have been adopted. The concentrated load $R_n$ is calculated, when the curve is continuous over the station points, as mentioned in equation 2 whereas, for junctions, when the load changes abruptly at the station points, the concentrated load (R) is calculated using $R_{nm}$ as mentioned in Eq. (5).

$$R_n = \frac{d}{12}(a + 10b + c) \quad \ldots (2)$$

where, $d$ is the distance between stations, $a$ and $b$ are the ordinates to $\frac{M}{EI}$ , $c$ is the extrapolated values (If for some reason, no actual values exists). The values obtained using Eq. (2 & 5) are fed in their respective rows in Table 2. For example, the value of the concentrated load $R_1$ at station 1 is determined from Eq. (3) as shown below:

$$R_1 = \frac{d}{12}(a + 10b + c) \quad \ldots (3)$$

$$= \frac{l/18}{12}[(0 + 10(1.838) + 3.459)]\frac{P\delta_1 l}{EI_3}$$

$$= 0.1011\frac{P\delta_1 l}{EI_3} \quad \ldots (4)$$

The same procedure can be successfully applied for the stations having continuous cross-section. For stations having an abrupt change in the $M/EI$ diagram, the fictitious reaction can be calculated as:

$$R_{nm} = \frac{d}{24}(7a + 6b - c) \quad \ldots (5)$$

For example, the value of the concentrated load $R_2$ at station 2 shown in Eq. (10) determined from Eq. (6 & 8) as shown below:

$$R_{21} = \frac{d}{24}(7a + 6b - c) \quad \ldots (6)$$

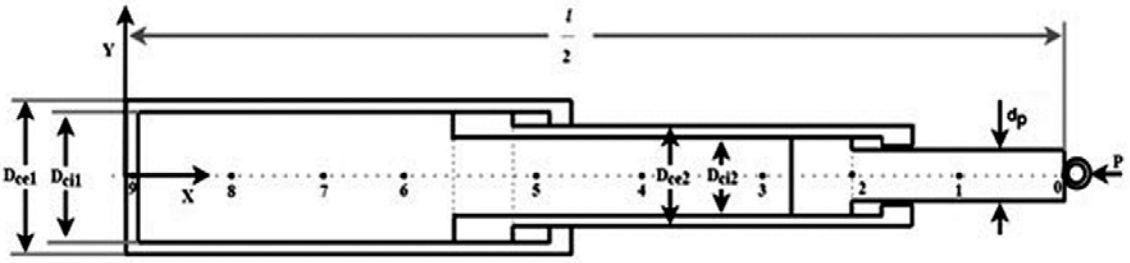


Fig. 1 — Half section view of the telescopic cylinder.

Table 1 — Dimension of the cylinder tube and piston rod.

| Hydraulic Cylinder | Diameter of tube 1(mm) | | Diameter of tube 2 (mm) | | Diameter of piston rod (mm) | Length of cylinder tube 1, $L_{c1}$ (mm) | Length of cylinder tube 2, $L_{c2}$ (mm) | Exposed length of piston rod, $L_p$ (mm) | Width of piston head, $L_{ch}$&$L_{ph}$ (mm) |
|---|---|---|---|---|---|---|---|---|---|
| | External $(D_{ce1})$ | Internal $(D_{ci1})$ | External $(D_{ce2})$ | Internal $(D_{ci2})$ | $(d_p)$ | | | | |
| | 72 | 60 | 60 | 48 | 24 | 535 | 495 | 485 | 21 |

Table 2 — Successive approximation method results.

| Station number | 0 | 1 | 2 | 3 | 4 | 5 | 6 | 7 | 8 | 9 | Common Factor |
|---|---|---|---|---|---|---|---|---|---|---|---|
| $y_1$ | 0 | 0.2099 | 0.3951 | 0.5556 | 0.6914 | 0.8025 | 0.8889 | 0.9506 | 0.9877 | 1 | $\delta_1$ |
| $M_1/EI$ | 0 | 1.838 | 3.459 1.378 | 1.938 | 2.411 | 2.799 0.8025 | 0.8889 | 0.9506 | 0.9877 | 1 | $\frac{P\delta_1}{EI_3}$ |
| R | | 0.1011 | 0.1252 | 0.1073 | 0.1336 | 0.0975 | 0.04927 | 0.0527 | 0.05476 | 0.05544 | $\frac{P\delta_1 l}{EI_3}$ |
| Average slope | | 0.7163 | 0.6101 | 0.2342 | 0.2117 | 0.1543 | 0.06228 | 0.06342 | 0.03778 | 0.01299 | $\frac{P\delta_1 l}{EI_3}$ |
| $y_{21}$ | 0 | 0.03582 | 0.06632 | 0.07803 | 0.08862 | 0.09633 | 0.09945 | 0.1026 | 0.1045 | 0.1052 | $\frac{P\delta_1 l^2}{EI_3}$ |
| $y_1/y_{21}$ | | 5.86 | 5.957 | 7.12 | 7.802 | 8.311 | 8.9738 | 9.265 | 9.445 | 9.506 | $\frac{EI_3}{Pl^2}$ |
| $y_{22}$ | 0 | 0.1767 | 0.3473 | 0.506 | 0.6487 | 0.7708 | 0.8691 | 0.9412 | 0.9852 | 1 | $\delta_2$ |
| $M_2/EI$ | 0 | 1.547 | 3.041 1.214 | 1.77 | 2.268 | 2.695 0.7708 | 0.8691 | 0.9412 | 0.9852 | 1 | $\frac{P\delta_2}{EI_3}$ |
| R | | 0.0857 | 0.1098 | 0.09806 | 0.1257 | 0.09344 | 0.04816 | 0.05216 | 0.0546 | 0.05542 | $\frac{P\delta_2 l}{EI_3}$ |
| Average slope | | 0.6031 | 0.5629 | 0.2343 | 0.2228 | 0.1723 | 0.07566 | 0.0741 | 0.04522 | 0.01521 | $\frac{P\delta_2 l}{EI_3}$ |
| $y_{33}$ | | 0.03016 | 0.0583 | 0.07002 | 0.08116 | 0.08977 | 0.09355 | 0.09726 | 0.09952 | 0.1003 | $\frac{P\delta_2 l^2}{EI_3}$ |
| $y_{22}/y_{33}$ | | 5.859 | 5.957 | 7.227 | 7.993 | 8.586 | 9.29 | 9.677 | 9.9 | 9.97 | $\frac{EI_3}{Pl^2}$ |

$$R_{21} = \frac{d}{24}[(7(3.459) + 6(1.838) - 0)]\frac{P\delta_1 l}{EI_3} = 0.08158\,\frac{P\delta_1 l}{EI_3} \quad \ldots (7)$$

$$R_{22} = \frac{d}{24}(7a + 6b - c) \quad \ldots (8)$$

$$R_{22} = d/24[(7(1.378) + 6(1.938) - 2.411)](P\delta_1 l)/(EI_3) = 0.04366(P\delta_1 l)/(EI_3) \quad \ldots (9)$$

$$R_2 = R_{21} + R_{22} = 0.1252\frac{P\delta_1 l}{EI_3} \quad \ldots (10)$$

The same procedure can be successfully applied for the stations having an abrupt change in the cross-section. This value is recorded in Table 2 as the fictitious shearing force or average slope. The fictitious reaction of the conjugate beam is:

0.1011 + 0.1252 + 0.1073 + 0.1336 + 0.0975 + 0.04927 + 0.0527 + 0.05476 + $\frac{1}{2}$(0.05544) = 0.7491

Now, the average slope is determined using a simple average method considering the different number of the station parameters.

Next, the deflection ($y_{21}$) in the system is calculated directly from the average slope, noting that the deflection at station 1 is equal to the value of average slope in the first segments times the distance between the stations, whereas, the deflection at station 2 is equal to the deflection at 1 plus the next values of average slope times the distance between the station *etc.*

For example, the value of the deflection ($y_{21}$) at station 1 is determined from the average slope as shown below in Eq. (11).

$$\frac{0.7163}{20} = 0.035815 \quad \ldots (11)$$

Similarly, the value of the deflection ($y_{21}$) at station 2 is determined asshown below in Eq. (12).

$$\frac{0.7163 + 0.6101}{20} = 0.06632 \quad \ldots (12)$$

The same procedure can be successfully applied to obtain the value of the deflection ($y_{21}$) for different stations. Finally, the ratio of the new values of ($y_{21}$)are obtained by using the assumed value of $y_1$. Considering the minimum and maximum values of the ratios, it can be seen from Eq. (13) that the lower and upper limits for critical load ($P_{cr}$) are obtained for 1st iteration cycle.

$$5.86\frac{EI_3}{l^2} < P_{cr} < 9.506\frac{EI_3}{l^2} \quad \ldots (13)$$

The piston rod has been proved to be more prone to buckling failure because of its less flexural rigidity[5]. Thus, from this point ahead, the buckling load for the system infers the buckling load for piston rod of the hydraulic cylinder.

As the length of each segment is constant for the given hydraulic cylinder, the ratio of $(y_1)_{av}$ to $(y_{21})_{av}$ is equal to the ratio of the sums of the deflection $y_1$ and $y_{21}$. Thus, the ratio of the sum of the deflection of 1st iteration cycle is shown in Eq. (14).

$$(y_1)_{av}/(y_{21})_{av} = ((2(0.2099 + 0.3951 + 0.5556 + 0.6914 + 0.8025 + 0.8889 + 0.9506 + 0.987) + 1)/(2(0.03582 + 0.06632 + 0.07803 + 0.08862 + 0.09633 + 0.09945 + 0.1026 + 0.1045) + 0.1052))\left(\frac{EI_p}{Pl^2}\right) \quad \ldots (14)$$

$$P_{cr} = 8.258\,\frac{EI_p}{l^2} \quad \ldots (15)$$

Further, substituting the original dimensions and the material properties in Eq. (14), $P_{cr}$ is determined as follows:

where

E = 220000 $N/mm^2$ $I_p = \frac{\pi}{64}d^4$ $d$ = 24 mm $l$ = 1501.5 mm

$P_{cr} = n * 8.258\frac{EI_3}{l^2} = 2 * 13110.833 = 26221.664$ N,

where $n$ is the number of stages.

The obtained result is improved by reiterating the cycle of calculation as shown in Table 2. The second cycle begins with deflection $y_{22}$ which is proportional to the deflection $y_{21}$ found from the first set of computations.

$$y_{22} = \frac{16\delta_2 x}{5l}\left(1 - \frac{2x^2}{l^2} + \frac{x^3}{l^3}\right) \quad \ldots (16)$$

where, $\delta_2$ equals the deflection at the centre of the hydraulic cylinder. In the next step, $M_2/EI_i$ are tabulated and represent the intensities of load on conjugate beam at the station points. These values are equal to $Py_{22}/EI_i$. Equation 17 shows the minimum and maximum values of the ratios, obtained for 1st iteration cycle that the lower and upper limits for load $P_{cr}$ lie between

$$5.859\frac{EI_p}{l^2} < P_{cr} < 9.97\frac{EI_p}{l^2} \quad \ldots (17)$$

Thus, the ratio of the sum of the deflection of 2nd iteration cycle is shown in equation 15. Equation 18 shows critical load for 2nd iteration cycle.

$$(y\_22)\_av/(y\_23)\_av = (((2 * (0.1767 + 0.3473 + 0.506 + 0.6487 + 0.7708 + 0.8691 + 0.9412 + 0.9852)) + 1)/((2 * (0.03016 + 0.0583 + 0.07002 + 0.08116 + 0.08977 + 0.09355 + 0.09726 + 0.09952)) + 0.1003))\left(\frac{EI_p}{Pl^2}\right) \quad \ldots (18)$$

$$P_{cr} = 8.576\frac{EI_p}{l^2} \quad \ldots (19)$$

Since the value is seen in Table 2, $P_{cr} = 9.97$ and thus it is seen that nearly accurate results have been obtained in the two-cycle of successive approximation computations. The numerical example is as shown below:

$$P_{cr} = n * 8.576\frac{EI_p}{l^2} = 2 * 13629.24 = 27258.48 \text{ N}$$

## 3 Finite element analysis

The finite element method (FEM) is a powerful approach, to reach a realistic solution which also reduced time, error efforts and cost. The specified pinned mounting hydraulic cylinder has been analysed by linear elastic static finite element analysis as presented in Fig. 2 using CAE package Abaqus.

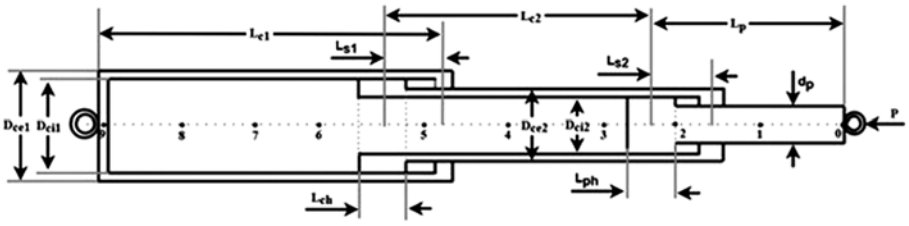


Fig. 2 — Schematic view of half of the hydraulic cylinder used in numerical simulation.

The linear elastic isotropic element has been considered for the finite element analysis of the hydraulic cylinder with Young's modulus E = 220000$N/mm^2$. Value of Poisson's ratio has been assumed to be 0.27 along with the mass density of 7.8*e-006. The structure can be well considered as a hinged beam having allowable rotation along z-axis at the cylinder tube 1 end and at the loading end rotation along with z-axis in combination with translational freedom along x- axis is considered. The eigenvalue buckling simulation has been performed for the full butt condition of the hydraulic cylinder. FEA model consists of 712 elements and 1207 nodes of linear hexahedral elements of type *c3d8r*. The modelled hydraulic cylinder is shown in Fig. 3.

The compressive load concentrated in nature has been applied at piston rod end and is increased stepwise from 1 N till the buckling is noticed. First, second and third buckling mode shapes obtained are shown in Figs 4, 5 and 6, respectively. Figure 7 shows the methodology adopted for the buckling load determination using Successive Approximation Method for two stage hydraulic cylinder. Table 3 enlists the buckling load for all three mode shapes.

Fig. 3 — CAD model of the considered telescopic cylinder.

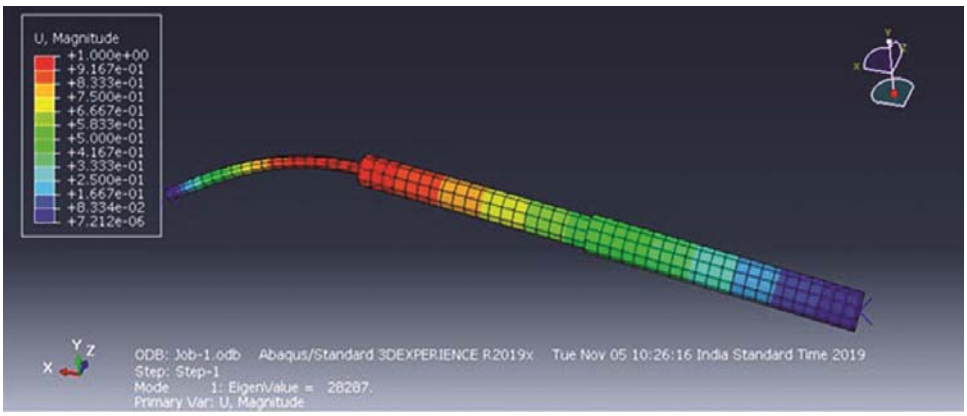


Fig. 4 — First buckling mode shape of the telescopic cylinder.


Fig. 5 — Second buckling mode shape of the telescopic cylinder.

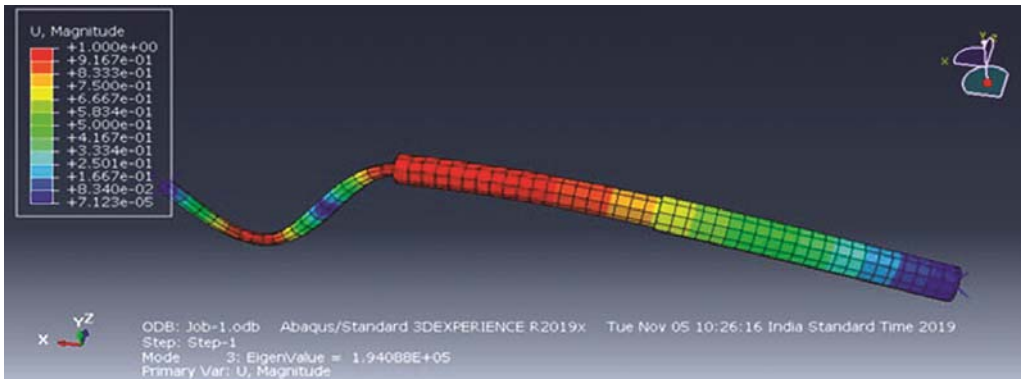


Fig. 6 — Third buckling mode shape of the telescopic cylinder.

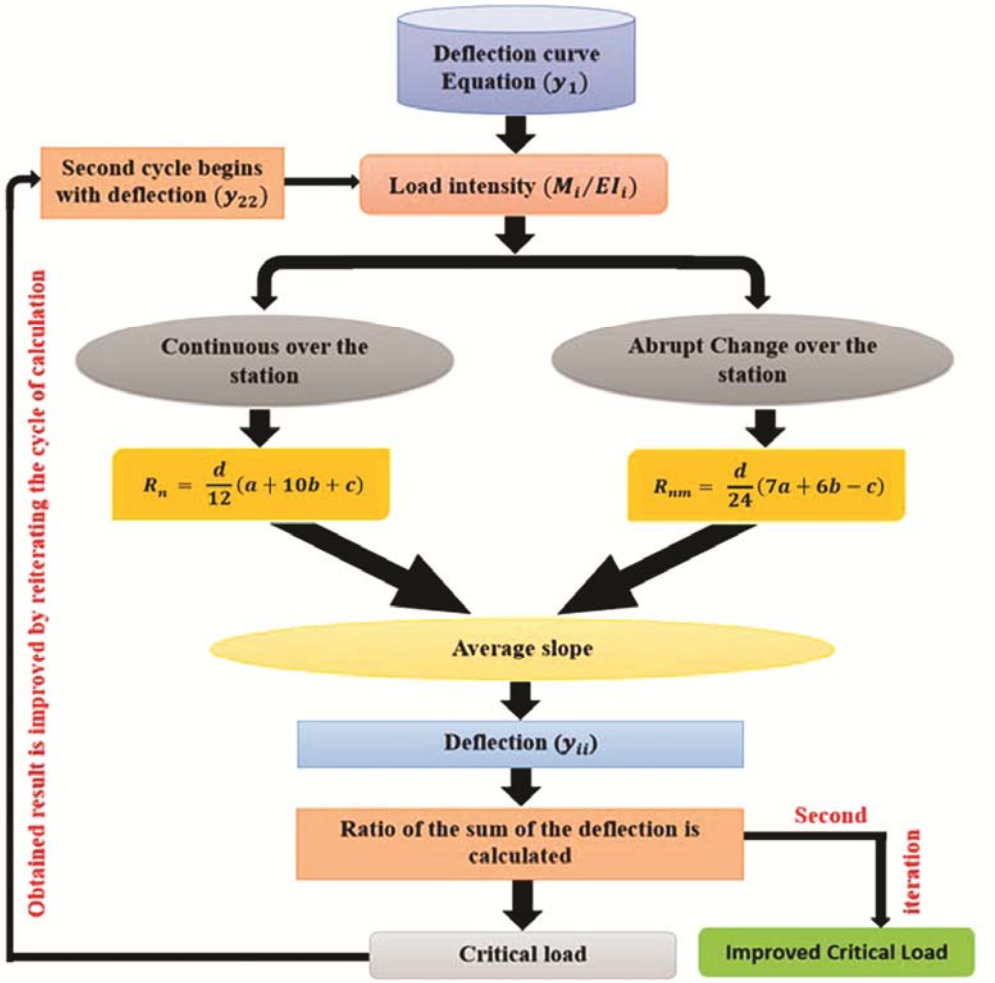


Fig. 7 — Flow chart of the methodology adopted for the successive approximation method.

Table 3 — Buckling load for different modes.

| Buckling mode shape | Buckling load (N) |
|---|---|
| First mode | 28287 |
| Second mode | 76529 |
| Third mode | 1.94088e+05 |

## 4 Conclusions

The overall finding of the proposed methodology can be listed as follows:

(i) The theoretical approximation of the buckling load of both ends hinged hydraulic cylinder has been

performed using a successive approximation method.

(ii) The study shows a good vicinity of the buckling load has been achieved in the second iteration of this method.

(iii) The numerical simulation has also been employed in order to validate the results obtained in this study.

(iv) The deviation of 3.63% has been noticed as per theoretical and numerical simulations.

(v) The outcomes of this method can be a more efficient way to determine the buckling load of a two-stage hydraulic cylinder for industrial purposes.

**Acknowledgements**

The authors would like to extend thanks to Mr Hirmukhe Sidram, Mr Akash Sharma, Ms Akanksha Chaudhari, & Mr Shivam Kumar of IIT, Indore, India for providing assistance during the research.

**References**

1 Hoblit F, *Product Engineering*, (1950) 108.

2 Flugge W, Stresses in shells (Springer Science & Business Media), ISBN 978-3-642-88291-3, 2013.

3 Seshasai K L, Dawkins W P & Iyengar S, *National Conf Fluid Power*, (1975).

4 Hydraulic fluid power-cylinders: A method for determining the buckling load, Tech. Rep. ISO/TS 13725, ISO Standard, (2001).

5 Prakash J, Aniket N, Kankar PK, Gupta VK, Jain PK, Ravinder T, Vinayak N & Ismail M, *Adv Eng Des*, Springer, (2019) 173.

6 Prakash J, Gupta S & Kankar P K, *Proc Institution Mech Eng, Part C: J Mech Eng Sci*, (2020) 0954406220916524.

7 Ramasamy V & Basha A J, *Defence Sci J*, 68(2) (2018) 167.

8 Timoshenko S, Theory of Elasticity (McGraw-Hill Education), ISBN 978-0070858053, 1970.

9 Shariati M, Sedighi M, Saemi J & Eipakchi H R, *Indian J Eng Mater Sci*, 17 (2010) 86.

10 Rao G V & Raju K K, *Indian J Eng Mater Sci*, 11 (2004) 143.